Hindawi
Journal of Chemistry
Volume 2020, Article ID 6279176, 9 pages
https://doi.org/10.1155/2020/6279176

Research Article

Effect of B_2O_3 Content on the Sintering Basic Characteristics of Mixed Ore Powder of Vanadium-Titanium Magnetite and Hematite

Hao Liu,[1,2] **Ke Zhang**,[1] **Qingfeng Ling**,[1] **and Yuelin Qin**[1,2]

[1]*School of Metallurgy and Materials Engineering, Chongqing University of Science and Technology, Chongqing 401331, China*
[2]*Value-Added Process and Clean Extraction of Complex Metal Mineral Resources, Chongqing Municipal Key Laboratory of Institutions of Higher Education, Chongqing 401331, China*

Correspondence should be addressed to Hao Liu; liuhao_023@163.com and Yuelin Qin; qinyuelin710@163.com

Received 21 March 2020; Revised 4 May 2020; Accepted 11 May 2020; Published 1 June 2020

Academic Editor: Nenad Ignjatović

The sintering basic characteristics of iron ore play a key role in the process of sintering. In this study, the effects of B_2O_3 on the assimilation characteristics, softening temperature, fluidity of liquid phase, compressive strength of bonding phase, and microstructure of the mixed fine powder of hematite and vanadium-titanium magnetite (H-VTM) are studied. Results show that B_2O_3 content from 0%–5% (wt%) could improve the assimilation characteristics of the H-VTM and increase the amount of the liquid phase. The liquidity of the bonding phase index (LBPI) of the H-VTM increases from 3.7 to 24.2. When B_2O_3 content exceeds 2%, the diameter of the pore in the H-VTM sintered samples enlarges. However, the compressive strength gradually decreases. Boron and calcium-magnesium-aluminium elements are abundant in the bonding phase, which can reduce the formation of calcium silicate and perovskite in H-VTM sintered samples.

1. Introduction

With the rapid development of the steel industry, the supply of high-quality iron ore is insufficient, so the vanadium-titanium magnetite (VTM) with sufficient reserves is highly needed. The extraction of iron, vanadium, titanium, and other elements in VTM has remarkably progressed, and its industrial-scale production is still dominated by the blast furnace ironmaking process. The primary raw materials for the blast furnace are vanadium-titanium sinter and vanadium-titanium pellets [1, 2].

Vanadium-titanium sinter is the raw material for the blast furnace, and there are still many difficulties in the production of vanadium-titanium sinter. As increasing the proportion of VTM in sintering, the amount of the liquid phase and the liquid-phase bonding force both decrease. Resulting in a lower yield and drum strength of vanadium-titanium sinter, the production volume of small size sinter also increases. Low-temperature reduction pulverization index ($RDI_{-3.15}$) of the vanadium-titanium sinter is significantly higher than the sinter without vanadium-titanium magnetite [3, 4].

Zhou et al. [5] revealed that enhancing granulation improved the breathability of the sintering layer, and the increase in oxygen potential could multiply the mass fraction of calcium ferrite in the sinter, including mineral composition, yield, and quality [6]. D. G. Jiang et al. [7] proposed a new idea based on the complementary mineralization of the assimilation characteristics and liquid phase fluidity. They confirmed the feasibility of mineralization based on the sintering basic characteristics of iron ore by optimizing the mineralization method and the sinter pot test. Xu et al. [8] confirmed that the low-temperature reduction pulverization index was improved, and the reduction index was enhanced by 2.6% when the content of iron concentrate rich in boron and magnesium in the vanadium-titanium sintering mixture approached 5%. Chu et al. [9–12] determined that economic indicators such as vertical sintering speed, yield, drum index,

sintering cup utilization coefficient, and low-temperature reduction pulverization index initially increased and subsequently decreased with increasing mass ratio of boron ore. Hao [13] found that the low-temperature reduction pulverization index and drum strength of the sintered ore increased, and the reduction index, softening temperature, and softening remain unchanged after boric acid and calcium chloride were added. Zhao et al. [14, 15] observed that adding a certain amount of boron-iron concentrate to the vanadium-titanium sinter could make full use of B_2O_3, as a result, the liquid phase of the sinter increased, the consolidation process improved, and the metallurgical properties of the sinter also enhanced.

Ren et al. [16, 17] researched the influencing pattern of different B_2O_3 contents on the mineral phase of high-titanium-type VTM and the qualities of sinter; they pronounced that B_2O_3 was mainly deposited in the $2CaO•xSiO_2•2/3\ (1-x)\ B_2O_3$ phase of vanadium-titanium sinter and B_2O_3 effectively inhibited the precipitation of $CaTiO_3$ and $2CaO•xSiO_2•2/3\ (1-x)\ B_2O_3$ and promoted the precipitation of iron-containing mineral phase.

In summary, we find that adding boron slime, boric acid, and boron-iron concentrate could improve the strength and the metallurgical performance of sinter and reduce the low-temperature pulverulent ratio, which is conducive to the blast furnace. It is not difficult to find that boron oxide plays a very important role in the sintering process. However, existing researches mainly focus on the effect of boron oxide on the macroperformance of vanadium-titanium sinter. Studies on the influence of B_2O_3 on the sintering basic characteristics of mixed ore powders using vanadium-titanium fine powder as the main raw material are rarely reported. Especially the researches on the influence mechanism of B_2O_3 on the sintering basic characteristics of mixed ore powder of vanadium-titanium magnetite and hematite have not been reported so far.

Hence, in this work, according to the actual production of mineral types and proportions in southwest China. Experimental samples are mixed with VTM concentrate and Australian hematite powder with a specific mass ratio (8 : 2), and this particular mixture powder is called H-VTM. The effects of B_2O_3 content on the assimilation characteristics, melting temperature, liquidity of liquid phase, compressive strength, and microstructure changes are studied. The influences of different B_2O_3 contents on the sintering basic characteristics of H-VTM sintering samples are obtained. The mechanism of B_2O_3 affecting the sintering process of vanadium-titanium magnetite and hematite is also clarified. Meanwhile, it is possible to find a new method for the recycling of B_2O_3 in boron-containing solid wastes.

2. Materials and Methods

2.1. Raw Materials. The chemical composition of the sintered raw material is shown in Table 1. Based on actual production situation, the mixed mineral powder used in this study composes of hematite powder and vanadium-titanium magnetite powder with a mass ratio of 2 : 8. The particle size of hematite powder and vanadium-titanium magnetite powder is both less than 74 μm. All the other reagents used in the experiments are of analytical grade.

2.2. Methods

2.2.1. Assimilation Characteristics. The assimilation characteristics experiment is shown in Figure 1. H-VTM and CaO are made into a mixed ore powder sample at 6000 N pressure, with a diameter of 8 mm and CaO sample with a diameter of 15 mm. The mixed ore powder sample was placed on top of the CaO sample and then placed into the sintering device to roast at 200°C in a specific heating system. The heating rate is 10° per minute until the end of the assimilation. Afterwards, the samples were naturally cooled and removed from the device. The assimilation characteristics were characterized at the temperature at which the contact angle between the H-VTM sample and the CaO sample began to change. The assimilation characteristics are used to characterize the difficulty of the reaction between iron ore powder and calcium oxide.

2.2.2. Melting Temperature. The experiment of melting temperature is shown in Figure 2. The chemical composition of the samples ensured the binary basicity R_2 of 2.0. A mixed sample (1.00 g) is placed in a 3 mm × 3 mm mould to make into the sample. Then, it is placed on a corundum gasket. The well-made sample is heated with a particular heating system; the melting of the column is observed to determine its melting temperature.

2.2.3. Compressive Strength of Bonding Phase. The experiment of the compressive strength of the bonding phase is shown in Figure 3. The chemical composition of the samples ensured the binary basicity R_2 of 2.0. Every mixed sample (3.00 g) is placed in a Φ8 mm × 8 mm mould. The samples are placed in the heating furnace under an air atmosphere and heated at 1250°C for 30 min. After heating, the specimens are moved out from the furnace and air-cooled to ambient temperature. Four sintered samples are selected for the compressive strength test. The average compressive strength is used to characterize the bonding phase strength.

2.2.4. Fluidity of Liquid Phase. The experiment of the fluidity is shown in Figure 4. The liquidity of the bonding phase index (LBPI) is calculated according to the equation as follows:

$$LBPI = S^* = \frac{S_1 - S_0}{S_0} \times 100\%, \quad (1)$$

where S^* represents the ratio of the increased area of the sample to the original area of the sample after heating and flowing and S_0 and S_1 are the vertical projection areas before and after flowing.

The chemical composition of the samples ensured the binary basicity R_2 of 2.0. A mixed sample of 1.00 g is placed in a Φ8 mm × 8 mm mould and heated at 1350°C for 30 min. After the samples cooled, every sample is removed and

Table 1: Chemical composition of ore powder (wt%).

Ore powder	TFe	SiO_2	CaO	Al_2O_3	MgO	TiO_2	MnO	FeO	P	S
VTM	55.78	4.33	0.69	3.86	2.78	9.08	0.36	30.50	0.09	0.54
Hematite	59.76	4.32	0.73	3.16	0.14	0.12	0.16	0.80	0.07	0.09
H-VTM	56.58	4.33	0.70	3.72	2.25	7.29	0.32	24.56	0.09	0.45

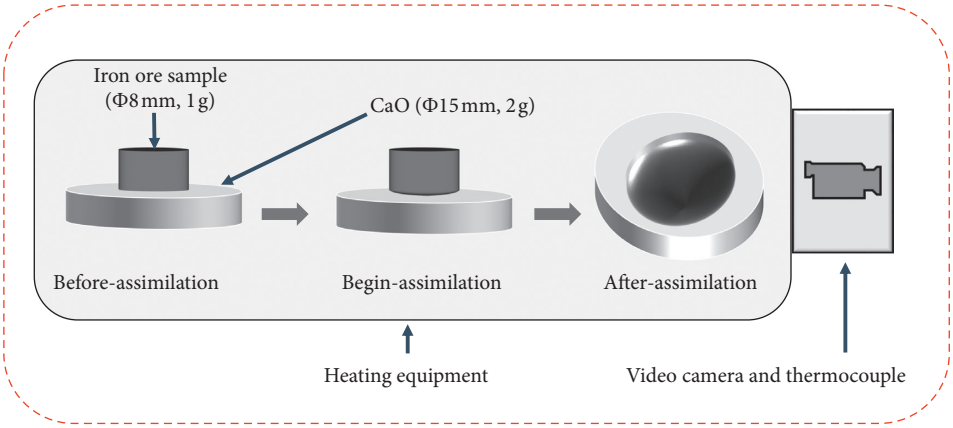

Figure 1: Diagrammatic chart of the assimilation characteristics experiment.

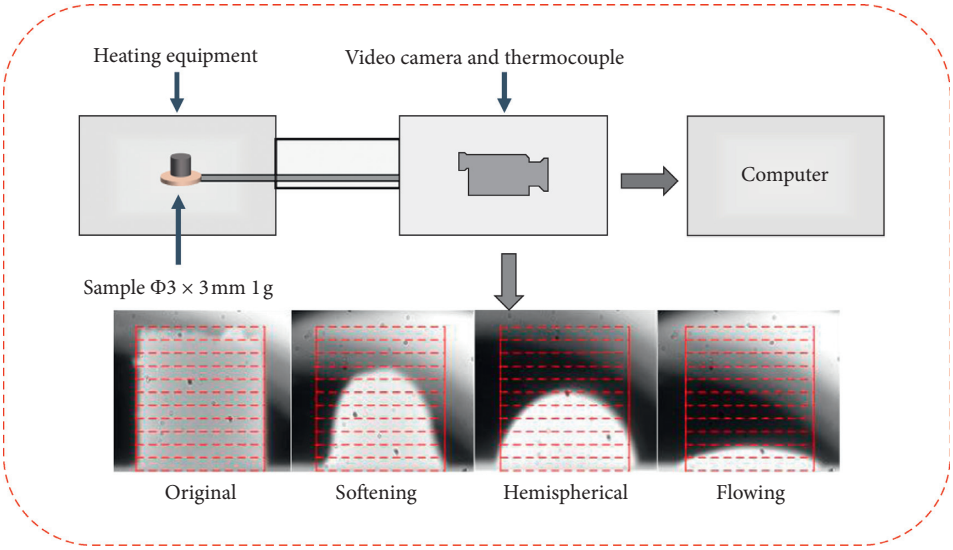

Figure 2: Diagrammatic chart of melting temperature experiment.

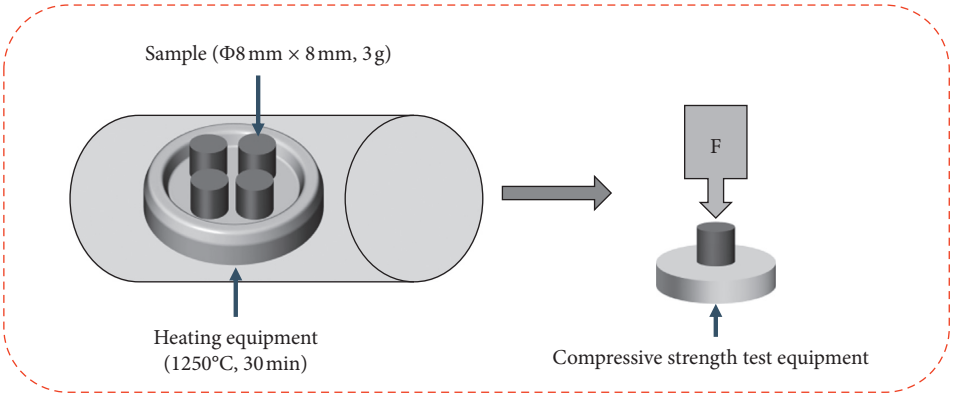

Figure 3: Diagrammatic chart of compressive strength of bonding phase.

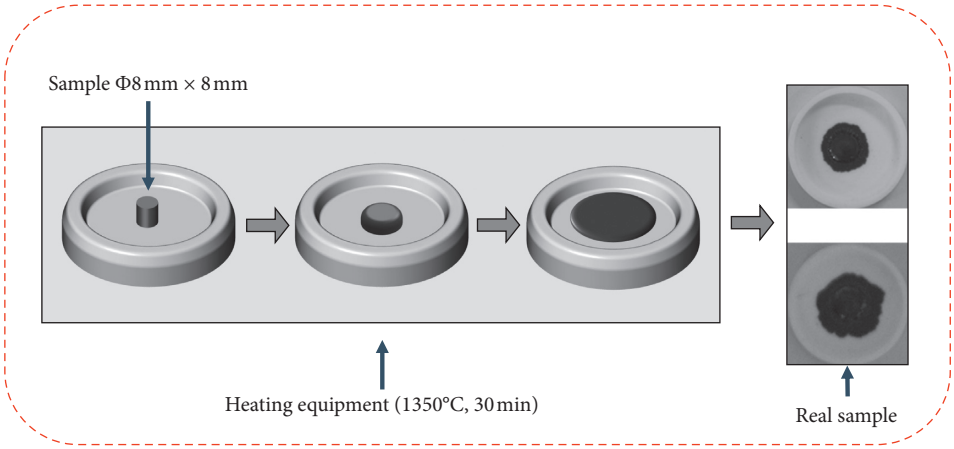

Figure 4: Diagrammatic chart of the fluidity of liquid-phase experiment.

analysed by image software. The fluidity of the bonding phase index of H-VTM samples is calculated according to equation (1).

3. Results and Discussion

3.1. Sintering Basic Characteristics of H-VTM with Different B_2O_3 Contents. In Figure 5, the sample without B_2O_3 began to assimilate at 1359°C, but the assimilation temperature decreased to 1205°C when the B_2O_3 was 5.00% (wt%). This result indicated that adding B_2O_3 could improve the assimilation characteristics of H-VTM. B_2O_3 has a low melting point (450°C), which could form a low-melting-point chemical compound and promote the formation of the liquid phase. For instance, the reaction of B_2O_3 with CaO and SiO_2 can form $2CaO{\cdot}B_2O_3{\cdot}SiO_2$ whose melting point is 901°C. This reaction could effectively inhibit the formation of calcium orthosilicate ($2CaO{\cdot}SiO_2$). B^{3+} is quickly diffused into the crystals of calcium orthosilicate ($2CaO{\cdot}SiO_2$) and inhibits multiphase transformation of calcium orthosilicate. This reaction is described in the subsequent microstructure analysis.

As is shown in Figure 5, when the mass ratio of B_2O_3 increased from 0.00% to 5.00%, the melting temperature decreased from 1504°C to 1453°C. When increasing the amount of B_2O_3, the melting temperature of H-VTM decreased obviously. In the whole process, adding B_2O_3 was conducive to the improvement of the capacity of the liquid phase inside the sintered samples. The LBPI of the H-VTM increased significantly from 3.70 to 24.2. This trend was consistent with the results which were calculated using the reaction module and the equilibrium module of FactSage 7.1 software. The calculation conditions were based on R_2 at 2.0 and carbon mass ratio at 3.5% under standard atmospheric pressure and air atmosphere. The chemical composition of the H-VTM was introduced in the reaction and the equilibrium module as input data. The amount of B_2O_3 was increased from 0.00% to 5.00% with a step size of 1.00%. The temperature was increased from 1000°C to 1600°C in a step of 50°C.

The average compressive strength of H-VTM fluctuated significantly with the rise of B_2O_3. The compressive strength was 531 N/P without B_2O_3. The compressive strength grew significantly with the increase of B_2O_3 content, peaking at 857 N/P with B_2O_3 content at 2.00%. As the B_2O_3 ratio further increases, the compressive strength dropped sharply, reaching its lowest point at 356 N/P with B_2O_3 ratio at 5.00%.

In Figure 6, at the same mass ratio of B_2O_3, the amount of liquid phase in sintering continuously increased with the increase of temperature, especially when the temperature exceeded 1210°C. At the same temperature, the amount of liquid phase of the sample with a high percentage of boron oxide was significantly more than the sample with lower ones. When the ratios of B_2O_3 were 0.00%, 1.00%, 2.00%, 3.00%, 4.00%, and 5.00%, the ratios of the liquid phase were 15.74%, 25.32%, 32.43%, 39.42%, 44.73%, and 51.36%, respectively. B_2O_3 could react with CaO, SiO_2, MgO, and Al_2O_3 to form mineral phases with a low melting point. Besides, the melting point of B_2O_3 is low (450°C). Therefore, B_2O_3 initially transformed into the liquid phase. Overheating reduced the liquid viscosity and quickly form a certain amount of liquid phase, which was beneficial for diffusion during sintering. As a result, the amount of liquid phase of H-VTM improved with the increase of the ratio of B_2O_3.

3.2. Microstructure of H-VTM with Different B_2O_3 Contents. The X-ray diffraction (XRD) is used to investigate the phases changes of the sintered samples. As is shown in Figure 7, after heating samples at 1250°C for 30 min, by contrast, the diffraction peaks of Fe_3O_4 and $CaO{\cdot}Fe_2O_3$ increased as the B_2O_3 mass ratio increased.

The addition of B_2O_3 could inhibit the formation of $2CaO{\cdot}SiO_2$ and promote the formation of $CaO{\cdot}Fe_2O_3$. This scene is shown in Figure 8. Before 1100°C, the $2CaO{\cdot}SiO_2$ content grew continuously with the increase of the B_2O_3 mass ratio. It reached its highest value when the addition amount of B_2O_3 is 5.00% at 1100°C.

The microstructures of the samples with different content of B_2O_3 were observed using a scanning electron microscope (SEM) equipped with an energy-dispersive X-ray spectroscope (EDS). In Figure 9, as the amount of B_2O_3 increased, the bonding phase (the bright white part) in the

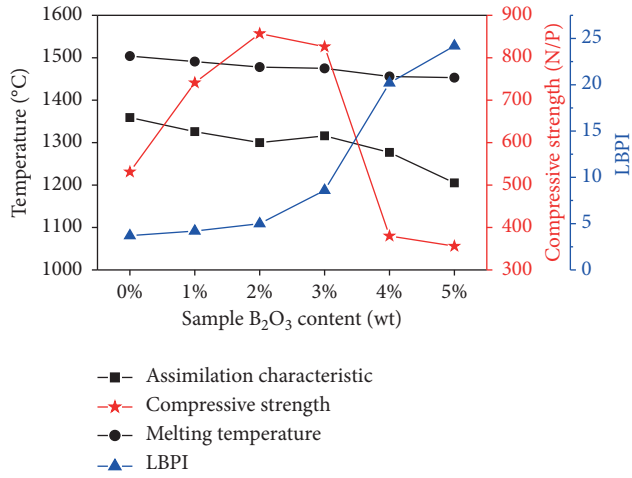

Figure 5: Sintering basic characteristics of the H-VTM sintered sample with different B_2O_3 contents.

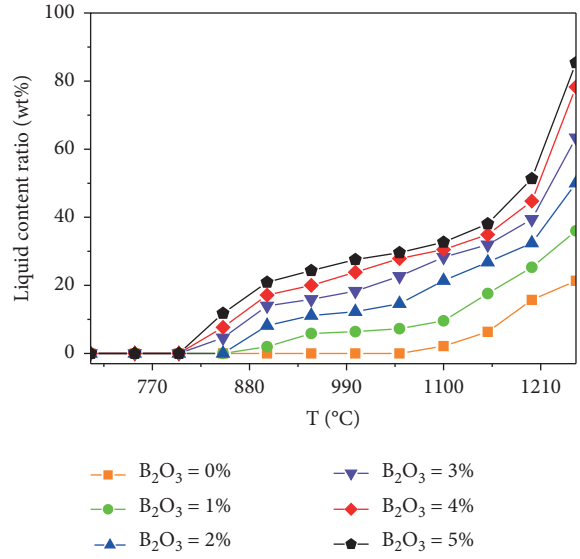

Figure 6: The volume of liquid phase with different B_2O_3 contents.

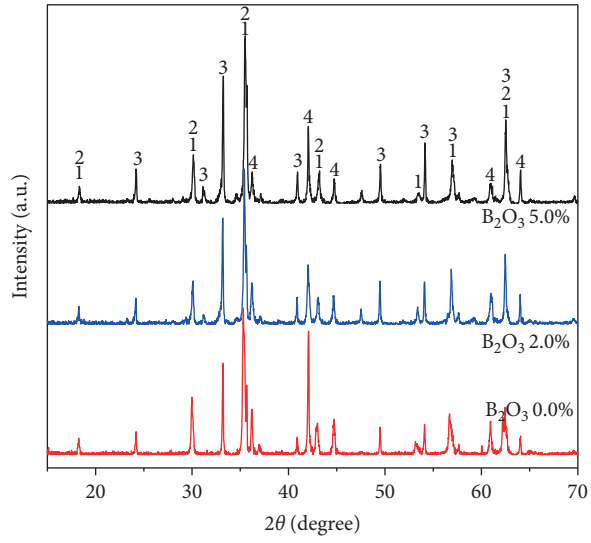

Figure 7: XRD patterns of H-VTM-sintered samples with different B_2O_3 contents. 1: Fe_2O_3; 2: Fe_3O_4; 3: $CaO{\cdot}Fe_2O_3$; 4: $2CaO{\cdot}SiO_2$.

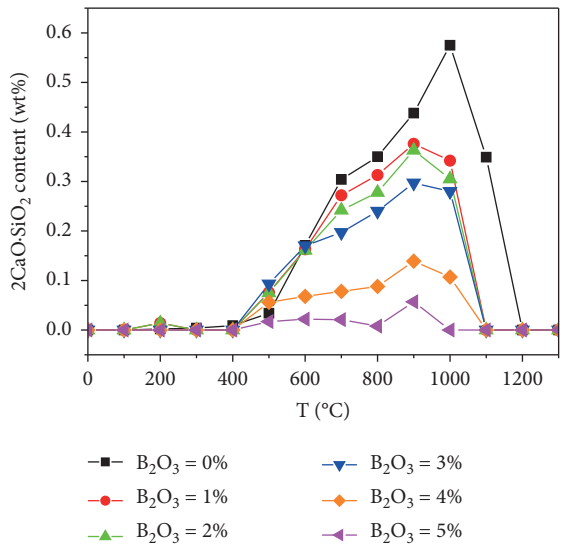

Figure 8: $2CaO{\cdot}SiO_2$ contents in the samples with different B_2O_3 contents.

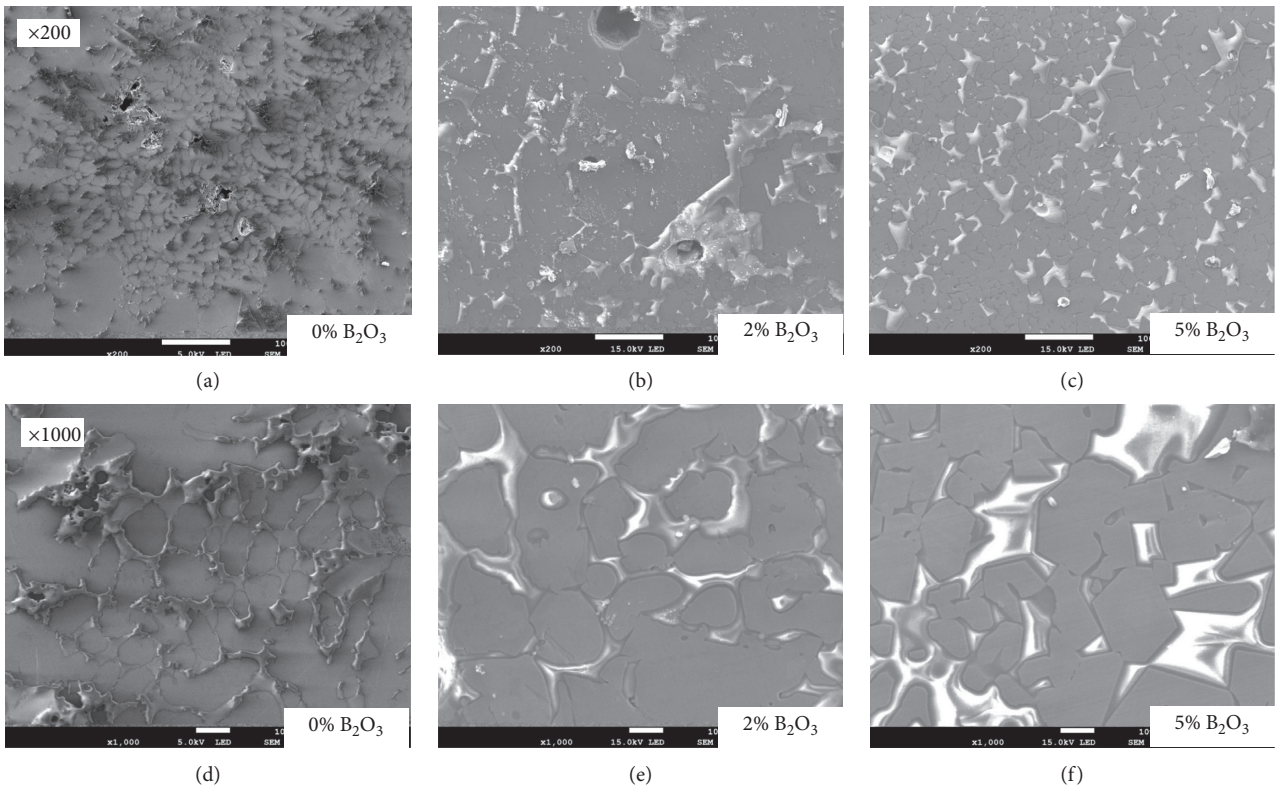

Figure 9: SEM of H-VTM with different B_2O_3 contents.

H-VTM-sintered sample was more evenly distributed in the microstructure. When the mass ratio of B_2O_3 was 2.00%, the number of pores in the sintered sample decreased significantly, but larger diameter pore began to appear because the increasing B_2O_3 could promote the formation of liquid phase in H-VTM. The liquid phase started to shrink during the cooling process and then came the pore structure. This phenomenon also could explain the inflexion point of the compressive strength of H-VTM and the increase of the number of internal pores, resulting in the formation of H-VTM microstructure and the decrease of compressive strength.

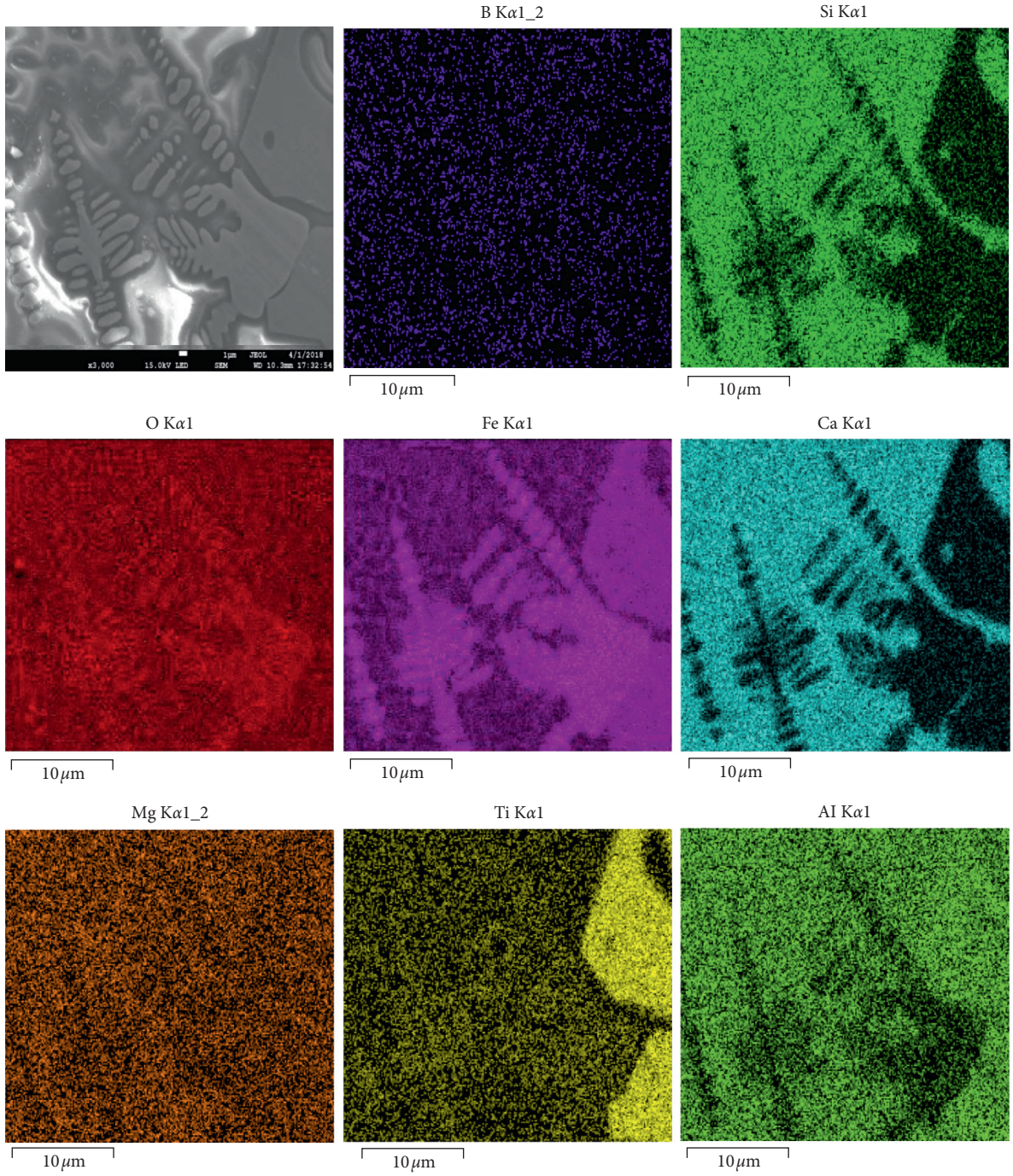

Figure 10: Surface scanning of the H-VTM sample with 5% B_2O_3.

The scanning results of the sintered sample with 5.00% B_2O_3 are shown in Figure 10. Hematite was mainly distributed in a fish-bone shape. Silicon, calcium, and aluminium were combined and distributed in the bright white area and formed a bonding phase. Titanium and iron were concentrated, producing the main iron base phase.

SEM-EDS was carried out on the cooled sample with 5.00% B_2O_3, as is shown in Figure 11. The EDS analysis results from point A to C with 5.00% B_2O_3 are shown in Table 2. The main element at point A is Fe, which accounts for 67.29%. O, Si, Ca, and other elements were almost nonexistent, which indicates that the main object is hematite or magnetite. The main elements at point B are O and Fe, and the contents of Si, Ca, and B are 6.14%, 14.35%, and 7.73%, respectively. Therefore, the primary material of the point B is ferrite, silicate, or borate, forming a bonding phase. Boron is abundant in the bonding material phase. As the B_2O_3 mass ratio increased, the perovskite phase decreased and calcium ferrite and calcium borate gradually increased, while calcium silicate gradually decreased. These results indicated that B_2O_3 worked together with CaO and SiO_2 to form the low-melting-point substance $CaO{\cdot}2B_2O_3$

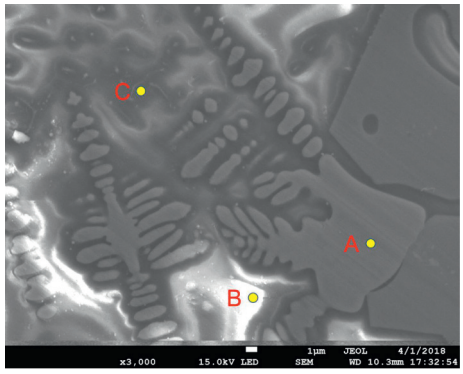

Figure 11: SEM-EDS of the sample with 5% B_2O_3.

Table 2: SEM-EDS analysis of the sample with 5.00% B_2O_3 (wt%).

Point	B	O	Fe	Si	Ca	Ti	Mg	Al
A	1.01	24.29	67.29	0.12	0.45	1.98	1.00	0.37
B	7.73	37.61	23.83	6.14	14.35	1.13	1.64	2.66
C	6.25	36.41	28.71	5.77	13.34	1.23	1.82	2.56

(melting point of 989°C), $CaO{\cdot}B_2O_3{\cdot}2SiO_2$ (melting point of 957°C), and $2CaO{\cdot}B_2O_3{\cdot}SiO_2$ (melting point of 901°C). Thus, the production of calcium silicate decreases, and this result is consistent with XRD.

4. Conclusions

The assimilation characteristics, melting temperature, fluidity of the liquid phase, compressive strength of the bonding phase, and microstructure of H-VTM with different B_2O_3 were studied through different methods:

B_2O_3 reduces the assimilation temperature of H-VTM and enhances its assimilation characteristics. As the amount of B_2O_3 increases, the melting temperature of H-VTM decreases, as well as LBPI. The addition of B_2O_3 can increase the amount of liquid phase and enhance the fluidity of the liquid phase.

B_2O_3 (<2.00%) improves the bonding phase strength of sintering samples, but the diameter of the pore in H-VTM enlarges when the amount of B_2O_3 is over 2.00% and the number of the pore increase. Thus, the H-VTM microstructure becomes more porous, and its compressive strength decreases.

Boron and calcium-magnesium-aluminium concentrated in the bonding phase can reduce the formation of calcium silicate and perovskite in the mixed samples of vanadium-titanium and hematite.

Data Availability

The data used to support the findings of this study are available from the corresponding author upon request.

Conflicts of Interest

The authors declare no conflicts of interest.

Authors' Contributions

Hao Liu, Ke Zhang, Qingfeng Ling, and Xinlong Wu contributed to perform the experiments, material characterization, data analysis, and paper writing. Yuelin Qin revised the paper and refined the language. Hao Liu and Yuelin Qin contributed to the design of the experiment.

Acknowledgments

This work was supported by the National Natural Science Foundation of China (Grant no. 51974054), Youth Project of Science and Technology Research Program of Chongqing Education Commission of China (no. KJQN201901), and China Scholarship Council (no. 201802075005).

References

[1] M. Zhou, S. Yang, T. Jiang, and X. Xue, "Influence of basicity on high-chromium vanadium-titanium magnetite sinter properties, productivity, and mineralogy," *JOM*, vol. 67, no. 5, pp. 1203–1213, 2015.

[2] J. Tang, Z. Yong, and M. S. Chu, "Effect of the increasing percentage of high chromium vanadium-titanium magnetite on quality of oxidized pellets," *Journal of Northeastern University*, vol. 34, no. 7, pp. 956–960, 2013.

[3] P. Gao, G. Li, X. Gu, and Y. Han, "Reduction kinetics and microscopic properties transformation of boron-bearing iron concentrate-carbon-mixed pellets," *Mineral Processing and Extractive Metallurgy Review*, vol. 41, no. 3, pp. 162–170, 2020.

[4] D. Jiang, "Mineral property and agglomeration intensification technology of vanadium and titanium magnetite concentrate," *Journal of Iron and Steel*, vol. 45, no. 1, pp. 24–27, 2010.

[5] M. Zhou, *Basic Research on Chromium-Containing Vanadium-Titanium Magnetite in the Sintering-Ironmaking Process*, Northeastern University, Boston, MA, USA, 2015.

[6] H. Liu, Y. Qin, X. Wu, and B. Xie, "Experimental study on oxygen-enriched sintering of vanadium-titanium magnetite," *Journal of Chemistry*, vol. 2018, Article ID 9342760, 9 pages, 2018.

[7] D. J. Jiang and M. G. He, "Experimental research on optimization matching ore proportioning of vanadium titanium magnetite concentrates," *Journal of Sichuan Metallurgy*, vol. 35, no. 1, pp. 20–27, 2013.

[8] J. C. Xu, Q. H. Pang, and J. W. Ma, "Influence of B on the microstructure of vanadium-titanium iron ore sintering," *Journal of University of Science and Technology Liaoning*, vol. 39, no. 6, pp. 401–405, 2016.

[9] M. S. Chu and Y. Tang, "Improving metallurgical properties of high chromium vanadium titanium sinter with bornite," *Journal of Northeastern University Natural Science*, vol. 12, no. 2, pp. 22–25, 2015.

[10] X. J. Fu and M. S. Chu, "Experimental study on preparation of oxidized barun iron ore pellets with boron-bearing iron concentrate addition," *Journal of Northeastern University Natural Science*, vol. 36, no. 1, pp. 52–56, 2015.

[11] S. Q. Chen, M. S. Chu, and Z. G. Liu, *Experimental Study on the Application of Boron and Magnesium Additives to Oxidized Pellet C*, 2009.

[12] J. L. Bai, J. L. Zhang, and S. Du, *Effect of Adding Boron-Iron Concentrate on Metallurgical Properties of Magnetite Pellets C*, 2013.

[13] D. S. Hao, *Study on the Experiment and Mechanism of Boracic Complex Additive to the Sinter*, Northeastern University, Boston, MA, USA, 2008.

[14] K. Zhang and Z. X. Yang, "Compressive strength and reducibility of B_2O_3-MgO-SiO_2-CaO-Fe_3O_4 agglomerate," *Journal of Northeastern University (Natural Science)*, vol. 18, no. 6, pp. 589–592, 1997.

[15] Q. J. Zhao, C. Q. He, and M. H. Gao, "Reasonable utilization of boronic magnetite ore," *Journal of Anhui University of Technology (Natural Science)*, vol. 14, no. 3, pp. 262–266, 1997.

[16] S. Ren, J. L. Zhang, X. D. Xing, B. X. Su, Z. Wang, and B. J. Yan, "Effect of B_2O_3on phase compositions of high Ti bearing titanomagnetite sinter," *Ironmaking & Steelmaking*, vol. 41, no. 7, pp. 500–506, 2014.

[17] S. Ren, J. L. Zhang, Q. C. Liu et al., "Effect of B2O3on reduction of FeO in Ti bearing blast furnace primary slag," *Ironmaking & Steelmaking*, vol. 42, no. 7, pp. 498–503, 2015.